Experimental determination of the rotational stiffness and moment capacity of connections in CLT buildings

Jenny Abrahamsson
Department of Building Technology,
Linnaeus University
Halmstad, Sweden

Filip la Fleur
Department of Building Technology,
Linnaeus University
Växjö, Sweden

Experimental determination of the rotational stiffness and moment capacity of connections in CLT buildings

1. Introduction

In Sweden, building with cross laminated timber (CLT) has become more favored during the last years. Due to the development of CLT-based building systems for multi-story buildings and due to higher loads, higher demands on the connections are required [1]. Since connections are used to transfer loads, connect members, and provide stiffness and ductility, the global structural behavior of a CLT structure is decisively affected by the behavior of the connections [2, 3, 4], especially in multi-story buildings.
In the structural analysis, of multi-story buildings, connections are commonly assumed to be pinned or rigid, even though the actual behavior is somewhere in between, i.e., semi-rigid [2]. For most structures adequate results can be achieved be assuming the connection to be rigid or pinned. This can however be a «problem» when designing taller CLT buildings where the stiffness in the connections is crucial [5]. Furthermore, the behavior of connections in timber structures can be described as ductile or brittle. Ductile behavior is characterized by the possibility to reach high deformations while still maintaining some of the strength in the connection, while for brittle behavior a sudden failure occurs at small deformations [6]. In CLT Buildings the ductile behavior is preferable [7].
Previous studies have focused on the compression perpendicular to the grain behavior [8], while knowledge about the rotational stiffness properties and the moment rotation behavior of wall-floor-wall connections in CLT-structures is currently limited and needs to be extended. Some work on the rotational stiffness and capacity of moment loaded steel to CLT contact connections was done in [9, 10]. Information on the rotational stiffness is crucial for a more efficient and reliable design of connections in CLT structures [2]. This research therefore focused on the rotational stiffness and moment capacity of common wall-floor-wall CLT connections in platform building systems.

2. Materials and methods

The rotational stiffness and moment capacity were studied through experimental investigations. The setup used in the experiments is shown in Figure 1 and the dimensions of the specimens for each series can be seen in Table 1. Different thicknesses of the CLT were used to investigate how the thickness of the wall and the floor specimens influence the stiffness and the moment capacity of the connection. In each of the four test series, eight replication tests were performed. The different CLT-layups used in the experimental campaign are shown in Table 2. Strength class C24 was used for all CLT elements. Prior to testing, specimens were stored in a climate room at constant temperature of 20 °C and a relative humidity of 65 %, resulting in a moisture content of about 12 %. The specimen was kept in the climate room until maximum one hour before testing of that specimen, in accordance to SS-EN 408 [11]. More information about specimen specifications and additional test series using screws and acoustic layers in the wall-floor-wall connection can be found in [12].

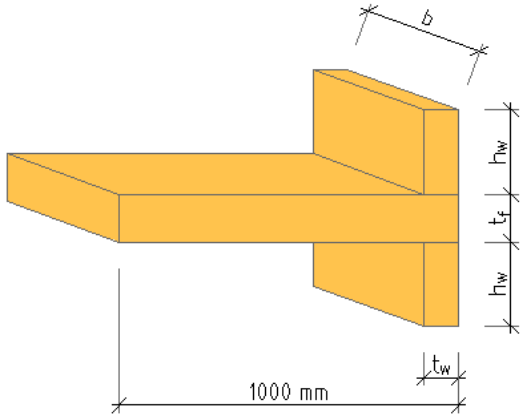

Figure 1: Nomenclature of dimensions for the CLT specimen.
Corresponding values for t_w, h_w, t_f and b are given in Table 1.

Table 1: Dimensions of the CLT specimens in each test series.

Test series	t_f [mm]	t_w [mm]	h_w [mm]	b [mm]
A	120 (5-layers)	80 (3-layers)	250	350
C	120 (5-layers)	140 (5-layers)	300	350
E	140 (5-layers)	100 (5-layers)	250	350
G	120 (5-layers)	100 (5-layers)	250	350

Table 2: Cross sectional dimensions of each CLT-layup.

Total thickness [mm]	Layer thickness [mm]
80	20-40-20
100	20-20-20-20-20
120	30-20-20-20-30
140	40-20-20-20-40

2.1. Test setup

The setup used during the tests is shown in Figure 2. For the application of the loading on the CLT wall element, and the CLT floor element, two pistons were used within a steel load frame. The pistons were placed with a distance of 800 mm between the center of each piston. The test setup was realized within a steel load frame with hydraulic actuators. The piston for load application on the wall was an MTS load actuator with a nominal force capacity of 500 kN and the piston for the floor load was an MTS load actuator with a force capacity of 250 kN. For uniformly load introduction, and to get a good contact surface between the pistons and the specimen, steel plates were used. The steel plates were meant to represent the contact from the continuation of the wall and the load application on the floor.

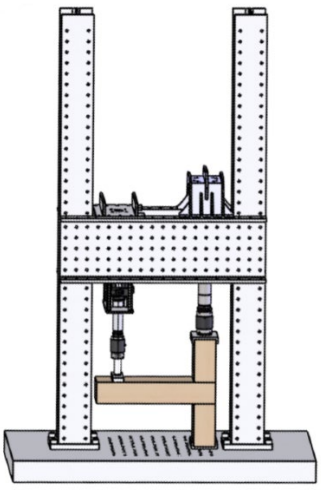

Figure 2: Test setup for the wall-floor-wall connection in the steel load frame.

The dimensions and the weight of the steel plates, which were located between the pistons and the CLT connection specimen, are given in Table 3. The steel plate used for load introduction on the CLT-floor element, to simulate a live load on the floor was a cuboid with a half-spherical hole on the upper side, providing the contact point for the piston. The reason for the spherical hole was used was to make sure that the steel plate was free to rotate at large displacements and thus to maintain contact with the floor specimen. Two sheets of teflon were put between the surface of the steel plate and the surface of the CLT floor specimen, to reduce friction and thus minimize horizontal load transfer between piston and CLT floor element (Figure 3).

Table 3: Dimensions of contact area and weight of steel plates used for load application.

	Weight [kg]	Length [mm]	Width [mm]
Floor	10.90	350	100
80 mm wall	15.64	350	80
100 mm wall	14.62	350	100
140 mm wall	12.34	350	140

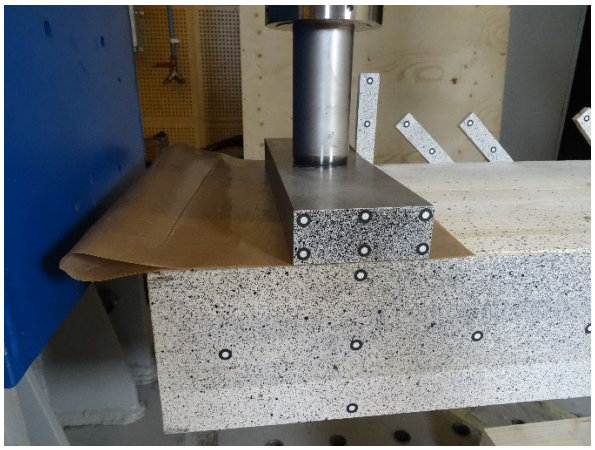

Figure 3: Teflon sheets in the test setup.

U-shaped steel plates were used for application of the pressure on the CLT wall element. The u-shaped allowed for horizontal stabilization, and thus to keep wall elements in place during assembly and testing of the CLT connections. The upper steel plate had a similar spherical hole on the top for load application through the piston, as it was used at the floor element. To secure the position of the CLT-elements, the plate for the lower wall had holes in the bottom, which were aligned to studs in the floor of the load frame.

2.2. Loading procedure

The same loading procedure was used for all tests (see Figure 4). As regards the loading on the wall, four different load levels were applied. These load levels corresponded to a contact pressure on the steel plate 0.5, 1.0, 1.5 and 2.0 MPa, corresponding to the weight of a different number of stories above the investigated wall-floor-wall connection. As soon as the force-controlled load level on the wall was applied, a relative displacement of 20 mm was applied on the floor element. The relative displacement started from the position of the floor piston after the load level on the wall was reached. During the test both pistons were always active. Hence, when the piston on the wall applied load, the floor piston kept a constant force, and vice versa when the floor piston moved displacement controlled to a certain displacement, the piston on the wall kept a constant force level.

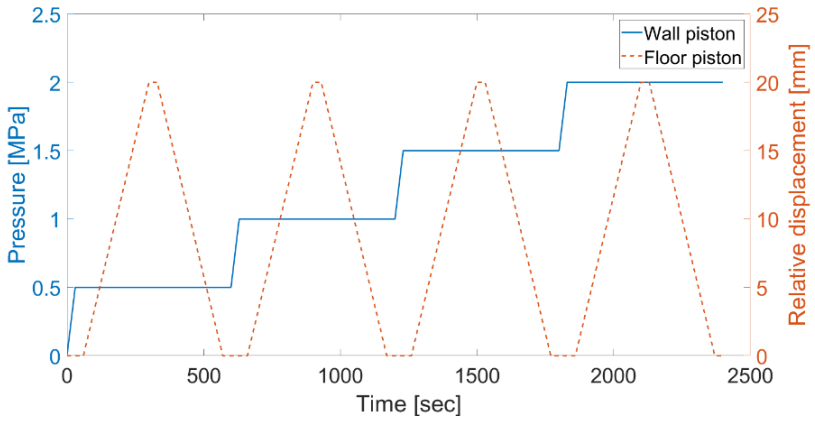

Figure 4: Loading procedure for the wall-floor-wall connection (idealized illustration).

At the start of the tests, pre-loads on the wall and floor element were applied. These pre-loads were small enough to not cause any damage to the specimen but still make the system stable. After the pre-loads had been applied and all the temporary supports had been removed, the test was started. Hence, the force on the wall was increased until the first load level of 0.5 MPa was reached. Thereafter the force was kept constant for 30 seconds to reduce the effect of creep deformations on the connection stiffness.
When the load on the wall was stable, i.e., after the 30 second holding phase, the piston on the floor started to move displacement controlled with displacement rate of 5 mm/min. After the 20 mm relative displacement had been reached there was a 30 second holding phase again to take the short-term creep into account and to reach stable load levels at the wall and floor piston. After these 30 seconds the unloading of the floor started. This was done with the same speed of 5 mm/min as for the loading phase. The unloading stopped when the load on the floor reached 100 N. Due to local plastic deformations in the material, the floor piston did not get back to the initial position. When 100 N had been reached in the unloading phase, there was once again a 30 second hold phase before the force on the wall was increased to a nominal stress of 1.0 MPa. After this the procedure was repeated for the four load steps.
All specimens used in the experimental part of the study were used twice. This was done to conduct as many tests as possible within the time frame of the research and with the available material. The wall elements were assumed to not be affected by the loading procedure since the wall was mainly loaded parallel to grain in the tests. The floor elements were also used twice as aforementioned. These elements were assumed to be affected in the contact area with the wall element, since loading was applied perpendicular to grain. Therefore, the floor elements were rotated 180° to be able to test both edges of the floor elements.

2.3. Load and deformation measurements

During each test, the deformations of the tested specimen were measured with an non-contact 3D optical measurement system, based on digital image correlation (DIC) (ARAMIS, GOM GmbH, Germany) [13]. The measurement system was used to document, analyze, and calculate the local material deformation. The deformations were further used to assess the displacement of specific points on the test specimen to be able to calculate the rotation of the floor. The applied forces from the pistons were measured by load cells of the MTS-hydraulic actuators and used as an analog input to the ARAMIS system. Detailed description of the ARAMIS setup can be seen in Section 3.4.3 in [12].
The displacement of specific points was measured with reference point markers placed on the specimen surface as shown in Figure 5. The reference point markers had an outer diameter of 10 mm including a white dot in the center with 5 mm in diameter. The placement of the markers was done in a symmetric pattern to be able to use the same marker when testing the other side of the floor specimen. On the backside of the specimen plywood sticks were attached with screws. These sticks had reference point markers on them to measure the displacement of the backside of the specimen. This was done to account for any torsional rotation of the floor specimen during testing. Figure 5 shows the position

of the markers for the test setup with 100 mm thick walls and a 120 mm thick floor. For the positioning of the reference point markers in the other configurations, the reader is referred to [12].

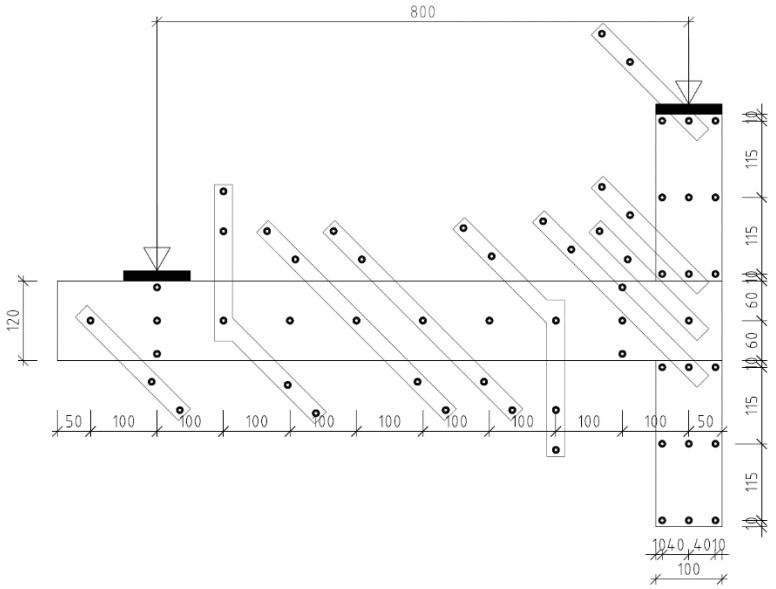

Figure 5: Illustration of distance between markers for test setup with 100 mm wall and 120 mm floor (dimensions in mm).

To get access to the local strains on the CLT surface in the connection area, a stochastic spray pattern was sprayed onto the front side of both the floor and wall specimens. The stochastic spray pattern and a detailed picture of the reference point markers are shown in Figure 6.

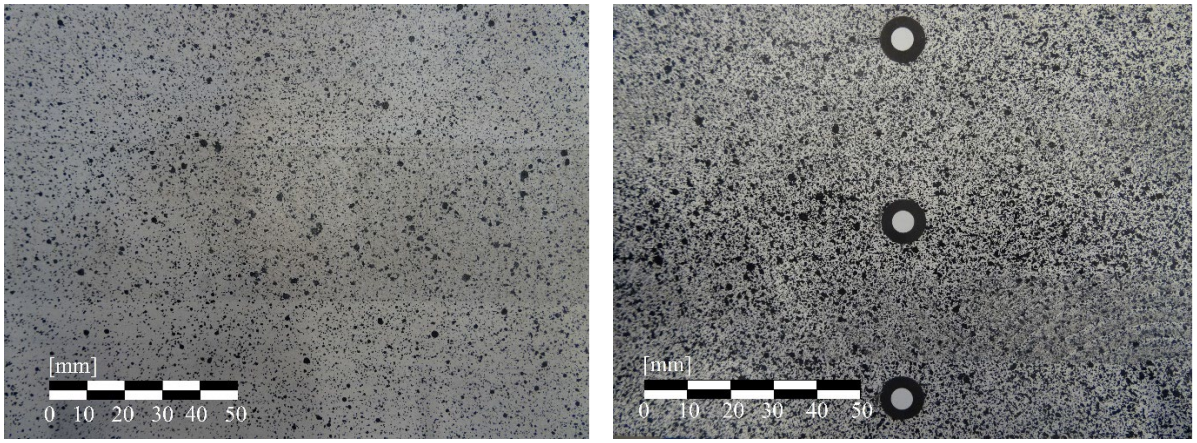

Figure 6: Spray pattern and the markers used on the specimens for DIC measurements.

2.4. Determination of moment capacity and rotational stiffness

The experimental data were used to calculate the rotational stiffness and moment capacity of the connection. This was done similar to the strength and stiffness determination for timber loaded in compression perpendicular to the grain as described in EN 408, by an iterative process as described in Section 2.4.5 [12]. A relative value of the rotation was used compared to the relative strain offset in EN 408, since results are expressed by moment-rotation curves created from the experimental data.
Instead of estimating the maximum compressive load, the maximum moment capacity was estimated. This estimation was set to start at a moment corresponding to a rotation of 0.02 rad. 10 % and 40 % of the estimated maximum moment capacity were then calculated to find the intersections points on the moment-rotation curve. A straight line was then drawn though these two intersection points and a parallel line was drawn with a distance of 0.01 rad along the rotational axis. This distance was assumed from the calculations of a 6 meter span beam with hinged connections and with a deflection of L/300.

The calculated maximum moment capacity was then determined by the intersection point of the second line with the moment-rotation curve. If the calculated value of the maximum moment capacity was within the tolerance of 0.5 % of the estimated value, the calculated value was then used to determine the maximum moment capacity. Otherwise, the procedure was repeated until a value of the maximum moment capacity was within the tolerance.

3. Results

3.1. Series A

In Figure 7 the moment-rotation curves for test series A are shown. Test series A was the test setup with 80 mm wall thickness and 120 mm floor thickness. The inclination of the curves change depending on the load level applied on the wall. A higher load level resulted in a higher inclination of the curve, and thus, in a higher rotational stiffness.

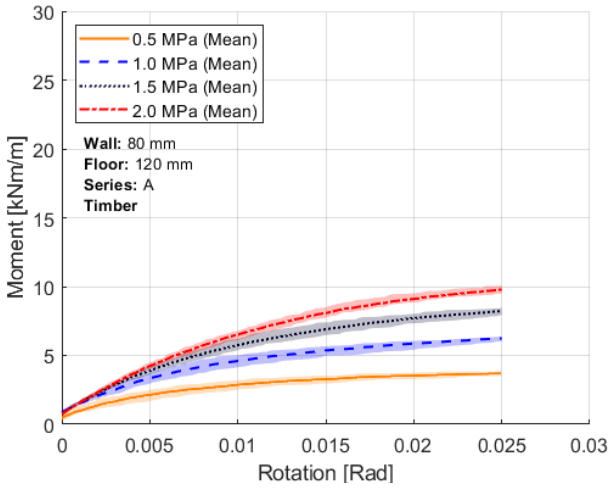

Figure 7: Moment-rotation curve for the four load levels in test series A. The shaded area behind the mean curves represents the interval between the minimum and maximum values of the individual tests.

In Table 4 the calculated mean moment capacity, rotational stiffness and the coefficient of variation (CV) for the different load levels in series A are summarized. The capacity and stiffness values are given per meter CLT wall/floor depth (b = 1 m). The capacity between load level 0.5 and 1.0 MPa increased with almost 70 % and the stiffness with just below 30 %. Between these two loads is the largest jump in percentage between two load levels. The increase from the lowest to the highest load level is for the capacity 175 % and for the stiffness 62 %.

Table 4: Moment capacity and rotational stiffness for the different load levels in series A.
The capacity calculated, based on the 0.01 rad offset.

Load level	Capacity [kNm/m]	CV [%]	Stiffness [kNm/rad/m]	CV [%]
0.5 MPa	3.42	4.90	434.86	31.64
1.0 MPa	5.78	3.40	565.06	16.57
1.5 MPa	7.76	2.36	667.97	7.83
2.0 MPa	9.43	2.05	706.29	3.93

An explanation for the CV for the rotational stiffness was thought to be because the moment-rotation curve levels out to almost a horizontal curve and therefore the same capacity from two tests can be found at very different rotations. This can also be seen as the variation is almost 10 times lower for the rotational stiffness of the 2.0 MPa load level compared to the 0.5 MPa load level. But at the same time the variation of the capacity only differs by a factor of approximately 2.5 between the two load levels.

3.2. Series C

In Figure 8 the moment-rotation curve for test series C are presented. Test series C was the setup with 140 mm wall thickness and 120 mm floor thickness. In this test setup the thickest walls of this study were used. This means that higher moments were needed to rotate the floor. Also, in this test series the inclination of the curves change depending on the load level applied on the wall. The curves in this test series do not end at the same rotation because of the bending of the floor element. For load levels of 1.5 MPa and 2.0 MPa the connection was stiff enough to cause significant bending deformations in the floor instead of almost pure rotation in the connection as it was seen for the lower load levels.

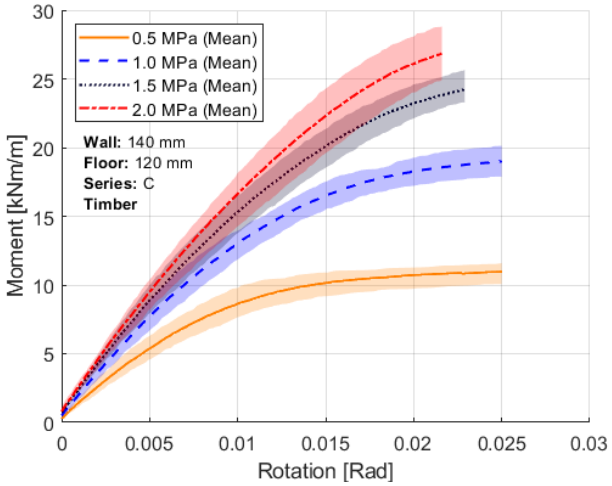

Figure 8: Moment-rotation curve for the four load levels in test series C. The shaded area behind the mean curve represents the interval between the minimum and maximum values of the individual tests.

In Table 5 the calculated mean moment capacity, rotational stiffness, and the CV for the different load levels in series C can be seen. Here the increase of both capacity and stiffness between the first and second load level are 75 % and 38 %, respectively. The increase from load level 0.5 to 2.0 MPa are 147 % and 62 % for the capacity and stiffness, respectively.

Table 5: Moment capacity and rotational stiffness for the different load levels in series C. The capacity calculated, based on the 0.01 rad offset.

Load level	Capacity [kNm/m]	CV [%]	Stiffness [kNm/rad/m]	CV [%]
0.5 MPa	10.71	5.19	1035.72	19.34
1.0 MPa	18.69	4.12	1426.30	12.52
1.5 MPa	23.69	4.81	1587.89	11.36
2.0 MPa	26.46	6.57	1678.46	9.98

In Figure 8 it can be seen, that just like for series A, there develops kind of a geometrical plasticity on the load level of 0.5 MPa. A thicker wall means that a greater moment was needed on the floor to lift the wall even if the same pressure was applied as for the 80 mm wall in series A.

3.3. Series E

In Figure 9 the moment-rotation curve for test series E can be seen. Test series E was the setup with 100 mm wall thickness and 140 mm floor thickness. The inclination of the curves change depending on the load level applied on the wall for this series as well. The moment-rotation curve shows a larger increase in the capacity between the load level of 0.5 and 1.0 MPa than it does between the other load levels, as it was seen for the previous series. The «geometrical plasticity» on the load level of 0.5 MPa can also be seen for this series.

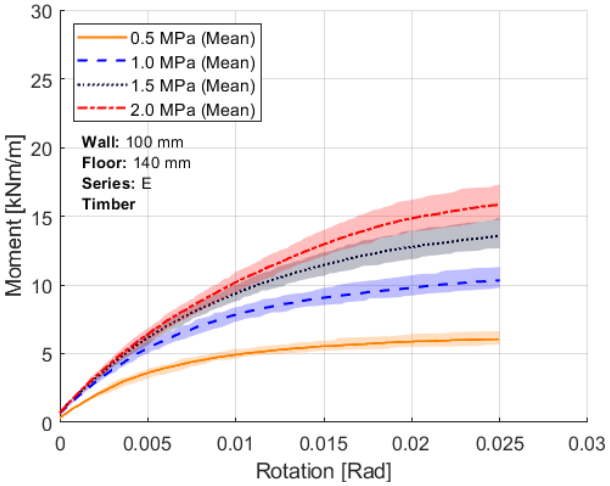

Figure 9: Moment-rotation curve for the four load levels in test series E. The shaded area behind the mean curve represents the interval between the minimum and maximum values of the individual tests.

In Table 6 the calculated mean moment capacity, rotational stiffness and the CV for the different load levels in series E can be seen. In this series the increase in capacity and stiffness between the load level of 0.5 and 2.0 MPa were 172 % and 47 %, respectively.

Table 6: Moment capacity and rotational stiffness for the different load levels in series E.
The capacity calculated, based on the 0.01 rad offset.

Load level	Capacity [kNm/m]	CV [%]	Stiffness [kNm/rad/m]	CV [%]
0.5 MPa	5.69	5.29	756.63	11.68
1.0 MPa	9.63	4.86	1029.89	6.97
1.5 MPa	12.92	5.52	1104.38	7.51
2.0 MPa	15.49	5.91	1112.41	7.82

The increase in stiffness between the load levels in this series align with the results from series A and C. In this series the variations are in general lower than compared with previous mentioned series. This could be because the bending stiffness in the specimen was higher than the other series and therefore does not influence the moment rotation curve as much.

3.4. Series G

In Figure 10 the moment-rotation curve for test series G can be seen. Test series G was the setup with 100 mm wall thickness and 120 mm floor thickness. In this series only four tests were used. As noticed in previous tests the connection stiffness dependents on the load level and increase with higher load.

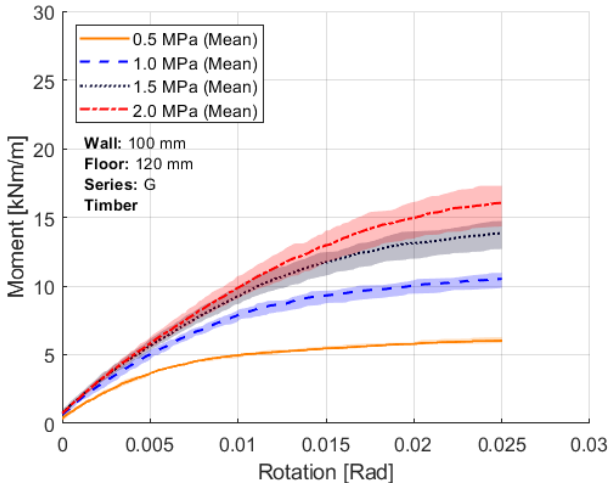

Figure 10: Moment-rotation curve for the four load levels in test series G. The shaded area behind the mean curve represents the interval between the minimum and maximum values of the individual tests.

In Table 7 the calculated mean moment capacity, rotational stiffness and the CV for the different load levels in series G can be seen. The increase in capacity and stiffness between the load level 0.5 and 1.0 MPa are in this series 81 % and 21 %, respectively. The total increase from load level 0.5 and 2.0 MPa for the stiffness and capacity are 175 % and 32 %, respectively.

Table 7: Moment capacity and rotational stiffness for the different load levels in series G. The capacity calculated, based on the 0.01 rad offset.

Load level	Capacity [kNm/m]	CV [%]	Stiffness [kNm/rad/m]	CV [%]
0.5 MPa	5.58	2.66	741.13	7.64
1.0 MPa	10.09	4.43	898.09	7.79
1.5 MPa	13.40	6.40	955.87	6.61
2.0 MPa	15.39	5.43	977.16	7.12

For more details on the result, the reader us referred to [12]. Furthermore [12, 14] include numerical models to calculate the stiffness of the tested connection.

3.5. Comparison

Two main things that can be noticed between the four series is that the biggest impact on the stiffness and capacity is the width of the wall. The wider the wall the higher capacity and stiffness of the connection. When looking at the influence from the thickness of the floor on the stiffness and capacity series E and series G where compared. Where the floor thicknesses were 120 and 140 mm, respectively. The difference is very small when looking at the capacity of the connection and only just above 10 % increase of the stiffness between the two floor thicknesses.
In Figure 11 a comparison between the capacity and stiffness depending on the thickness of the wall can be seen. In the graphs the blue line, line drawn between the boxplots, represent the mean value between the different test series. The red line in each box is the median of that specific series. Furthermore, the values inside the boxes represent the values between the 25 and 75 percentiles. Finally, the outer lines represent the maximum and minimum values. Linear regression was used to create the equations based on the results. A coefficient of determination (R^2) was calculated for all the linear regressions. The R^2 show how strong the linear relationship between the variables is, in this case the thickness of the wall and moment capacity or rotational stiffness. For all the load levels the moment capacity can be considered linear depending on the thickness of the wall.

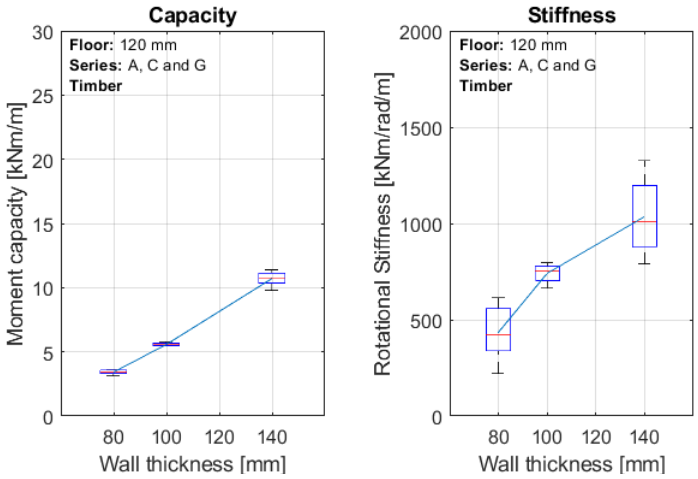

Figure 11: Box plot of the moment capacity and rotational stiffness depending on the thickness of the walls for load level 0.5 MPa.

For load level 0.5 MPa both the moment capacity and rotational stiffness were given equations to estimate the moment capacity and rotational stiffness based on the thickness of the wall. The equations for the estimations can be seen in Eq. 1 and 2, respectively.

$$M_{R,0.5} = 0.122t_w - 6.424, \quad (1)$$

$$K_{R,0.5} = 9.784t_w - 320.2, \quad (2)$$

where $M_{R,0.5}$ is the moment capacity in kNm/m, $K_{R,0.5}$ is the rotational stiffness in kNm/rad/m and t_w is the thickness of the walls in mm. For Eq. (1) and (2) the R^2 values are 0.988 and 0.755, respectively.
The other main result that can be seen throughout the four test series is that the load level impact both the capacity and the stiffness. The capacity had an increase with around 150 % or higher in all four series and the stiffness had an increase between 32 and 62 %. The variation between the tests was in general lower for the capacity than it was for the stiffness in all of the series.

4. Conclusions

In the study 28 tests in four different series were performed. The series differed with different wall thicknesses and floor thicknesses. The testing procedure was the same for all of the four series and included for different load levels on the wall and a 20 mm deformation of the floor element.
The two main factors, influencing the behavior of the connection was the load level on the wall and the thickness of the wall. For the series with 80 mm wall and 120 mm floor the increase in capacity and stiffness was 175 % and 62 % respectively when increasing the load from 0.5 MPa to 2.0 MPa. For the difference between the wall thickness an increase in capacity and stiffness of 213 % and 137 % could be seen when comparing the 80 and 140 mm walls when looking at a load of 0.5 MPa.
It was also seen that the connection showed a ductile behavior. This was seen by the large deformations that were achieved in the test series, without and brittle failure.

5. References

[1] M. Izzi, A. Polastri, and M. Fragiacomo. Modelling the mechanical behaviour of typical wall-to-floor connection systems for cross-laminated timber structures. *Engineering structures*. vol. 162, pp. 270–282, 2018. [Dataset]. Available: http://doi.org.10.1016/j.engstruct.2018.02.045.

[2] G. Flatscher. Evaluation and approximation of timber connection properties for displacement-based analysis of CLT wall systems. *Timber Engineering Technology*. vol. 6, 2017. [Dataset]. Available: http://dx.doi.org/10.3217/978-3-85125-557-7.

[3] I. Gavric M. Fragiacomo A. Ceccotti. Cyclic behavior of typical screwed connections for cross-laminated (CLT) structures. *European Journal of Wood and Wood Products*. vol. 73, pp. 179–191, 2015. [Dataset]. Available: https://doi.org/10.1007/s00107-014-0877-6.

[4] R. Brandner et al. Cross laminated timber (CLT): overview and development. *European Journal of Wood and Wood Products*. vol. 74, pp. 331–351, 2016. [Dataset]. Available: https://doi.org/10.1007/s00107-015-0999-5.

[5] S. Tulebekova, K. A. Malo, A. Rønnquist, and P. Nåvik. Modeling stiffness of connections and non-structural elements for dynamic response of taller glulam timber frame buildings. *Engineering Structures*, 261:114209, jun 2022. ISSN 01410296. doi: 10.1016/j.engstruct.2022.114209. URL https://linkinghub.elsevier.com/retrieve/pii/S014102962200339X.

[6] A. Jorissen and M. Fragiacomo. General notes on ductility in timber structures. *Engineering Structures*. vol. 33, pp 2987–2997, 2011. [Dataset]. Available: http://dx.doi.org/10.1016/j.engstruct.2011.07.024.

[7] H. J. Blaß and P. Schädle. Ductility aspects of reinforced and non-reinforced timber joints. *Engineering structures*. vol. 33, pp. 3018–3026, 2011. [Dataset]. Available: https://doi.org/10.1016/j.engstruct.2011.02.001.

[8] M. Schweigler et al. An experimental study of the stiffness and strength of cross-laminated timber wall-to-floor connections under compression perpendicular to the grain. *Engineering Structures*. vol. 271, 114850, 2022. [Dataset]. Available: https://doi.org/10.1016/j.engstruct.2022.114850.

[9] M. Schweigler, T.K. Bader, and S. Sabaa. Design of moment loaded steel contact connections at the narrow face and side face of CLT panels. *In: 9th INTER Proceedings: International Network on Timber Engineering Research, 55-7-7, Bad Aibling, Germany, August 22-25, 2022.*

[10] M. Schweigler et al. Non-uniform compressive loading of cross-laminated timber (CLT) perpendicular to the grain. *In Proceedings of the World Conference on Timber Engineering* (WCTE 2021), [Online]. 2021.

[11] *SS-EN 408:2010+A1:2012: Timber structures – Structural timber and glued laminated timber – Determination of some physical and mechanical properties*. Swedish Standards Institute (SIS), Stockholm, Sweden, 2012.

[12] J. Abrahamsson and F. la Fleur. The impact of connection stiffness on the global structural behavior in a CLT building. M.S. Thesis, Dep. of Building Technology, Linnaeus University, Växjö, Sweden, 2021. [Online]. https://www.diva-portal.org/smash/get/diva2:1570139/FULLTEXT01.pdf.

[13] *GOM. GOM Correlate Professional – V8 SR1 Manual Basic*. Braunschweig, Germany: GOM GmbH. 2015. [Dataset]. Available: http://213.8.45.88/PDF/gom_correlate_prof_basic_v8.pdf. (Visited on 04/08/2021).

[14] S.T. Akter, T.K. Bader, and E. Serrano. Stiffness of cross-laminated timber (CLT) wall-to-floor-to-wall connections in platform-type structures. *In Proceedings of the World Conference on Timber Engineering* (WCTE 2020), [Online]. 2021.